Soft Matter

Controlling protein adsorption modes electrostatically

Journal:	*Soft Matter*
Manuscript ID	SM-ART-04-2020-000632.R2
Article Type:	Paper
Date Submitted by the Author:	19-May-2020
Complete List of Authors:	Dahal, Yuba; Northwestern University, Material Science and Engineering Olvera de la Cruz, Monica; Northwestern University, Materials Science and Engineering

Journal Name

ARTICLE TYPE

Cite this: DOI: 10.1039/xxxxxxxxxx

Received Date
Accepted Date

DOI: 10.1039/xxxxxxxxxx

www.rsc.org/journalname

Controlling protein adsorption modes electrostatically

Yuba Raj Dahal[a] and Monica Olvera de la Cruz[a,b,c,*]

Protein adsorption on surfaces is ubiquitous in biology and in biotechnology. There are various forces required for controlling protein adsorption. Here, we introduce an explicit ion coarse–grained molecular dynamics simulation approach for studying the effects of electrostatics on protein adsorption, and $2D$ protein assembly on the charged surface. Our model accounts for the spatial distribution of protein charges. We use catalase as our model protein. We find that the preferential adsorption mode of proteins at low protein concentration on a charged surface is "standing up". When the protein concentration in a solution increases to reach a critical density on the surface, the adsorption mode switches from "standing up" to a mixed state "flat on" and "standing up", which increases the lateral correlations among the adsorbed proteins. As such, the changes in the adsorption mode arise from the protein adsorption that cancel the surface charge and the protein–protein repulsion. This correlated surface structure melts as the salt concentration increases because the charged surface is cancelled by the salt ions and the proteins de–adsorb. For the case of strongly charged surfaces the "standing up" conformation remains more favorable even at high protein adsorption at low salt concentrations since in that conformation the surface charge is cancelled more effectively, generating an even more laterally correlated structure. We elucidate the effects of parameters such as surface charge density, salt concentration, and protein charges on the different adsorption modes and the structure and organization of proteins on the charged surfaces. This study provides a guide for controlling protein assembly on surfaces.

1 Introduction

Protein adsorption is encountered in life and physical sciences as well as in industry, biotechnology and medicine. Understanding the process of protein absorption to a surface is of particular importance since the biological function of proteins is strongly affected by the surface [1–3]. Moreover, protein adsorption can cause detrimental outcomes. For example, the adsorption of proteins on biomedical implants in contact with the blood may lead to a blood clot, and obstruct blood flow causing thrombosis [4,5]. In artificial tissue scaffolds, on the other hand, adsorption of proteins is a requirement for proper vascularization [6,7]. The interplay between forces of different origin such as electrostatic, depletion, and hydrophobicity determines the extent of protein adsorption. However, studies examining the effect of these forces on protein adsorption are challenging, because proteins have heterogeneous chemical surface compositions and asymmetric shapes. Also, protein forces depend upon several external parameters such as solution pH, salt types, and concentration [8–10], etc.

There are numerous experimental, theoretical and simulation studies on protein adsorption on surfaces [11–15]. Most theoretical studies account for the overall net charge of the protein and are generally limited to a low concentration of proteins. This omits the contributions of the spatial distribution of the protein's residues on the adsorption. On the other hand, consideration of a few proteins in all atom simulation leaves out correlation effects in the adsorption. Simple anisotropic molecules are expected to land on the surface via their largest interface. However, in the case of proteins, the adsorption interface may differ from the anticipated adsorption interface as a result of their charge heterogeneity. Once proteins are within close proximity to the surface, local interactions between the protein's residues and the surface come into play, which, in turn, play a major role in determining the adsorption interface. In addition, correlations between proteins on the surface is another key player for affecting the adsorption modes of proteins. In this study, we take into account both the protein charge distribution, and many body interactions in the model.

Here, we develop a coarse–grained molecular dynamics (MD) simulation approach to elucidate the effects of protein charge, surface charge density, protein concentration, and salt concentration on the protein adsorption mode, and $2D$ protein structures on the charged surfaces. At low protein solution concentration,

[a] Department of Material Science and Engineering, Northwestern University, Evanston, Illinois 60208, United States
[b] Department of Chemistry, Northwestern University, Evanston, USA
[c] Department of Physics and Astronomy, Northwestern University, Evanston, USA
* m-olvera@northwestern.edu

we find that the preferential adsorption mode of a protein is *via* the smallest interface contact (termed here "standing up", shown in fig 1). Our analysis suggests that the mode of protein adsorption onto the surface is determined by a local interaction between protein and surface. We increase the protein solution concentration to find the critical density on the surface for changing the protein adsorption from "standing up" to "flat on" (adsorption *via* the largest interface contact) mode. We also analyze the effects of surface charge density, salt concentration, and protein charges on the adsorption interface, and protein assemblies on the charged surface. At intermediate values of protein charges ($-12|e|$), the surface charge density increment changes the protein adsorption from "standing up" to "mixed" (a combination of "standing up" and "flat on") and back to "standing up" mode again. These changes induce the structural transformation of the $2D$ protein assembly from a poorly correlated sparse $2D$ structure to a densely packed structure having hexagonal symmetry. When the proteins are strongly charged ($\sim -20|e|$), we observe ordered structures only at low surface charge densities. Under an increasing salt concentration, we observe that a dense hexagonal structure changes into a sparse structure, which on further increasing the salt concentration dissolves into the bulk solution. This study provides a useful guide for understanding protein adsorption, and the $2D$ assembly of proteins on surfaces.

2 Model and simulation details

Bovine liver catalase (pdb code: $1TGU$)[16] is used as our model protein. This is a tetrameric enzyme that plays a critical role in maintaining safe levels of hydrogen peroxide in the cell[17]. In addition to its importance in biology, catalase enzyme has a wide range of applications in industry including food and textile, to name a few[18]. People have used catalase enzyme for constructing multi-component enzyme superlattices[19] and mixed protein-gold superlattices as a function of salt concentration[20] as well as the degradation of DNA[21]. In this coarse–grained model, a coarse-grained bead is used to represent each amino acid of the protein, and to accurately mimic the shape and surface roughness of the protein. More importantly, the *CG* beads capture the spatial distribution of the protein's charges precisely. In a simpler geometric form, heterogeneous face charges can be placed using approximations. However, those heterogeneous face charges will be insufficient to represent the spatial distribution of protein charges, which is crucial in determining the mode of protein adsorption. Also, the excluded volume interaction, proteins contacts and alignments on surfaces can more realistically be captured with this CG than using a simpler geometry. We assign positive charges to *CG* beads representing *Arg* and *Lys* amino acids, and negative charges to beads that represent *Asp* and *Glu* residues. The charge states of amino acids at different *pH*s are calculated from the Henderson–Hasselbalch equation using average *pKa* values[22]. The charges assigned to negatively charged residues (*Glu* and *Asp*) at various solution *pH*s are tabulated in tab.(1). In *pH* range $4.0-7.0$, partial charges of positively charged residues are larger than $0.99|e|$. Therefore, we assign $+1|e|$ charge to each of them.

Table 1 Partial charges assigned to negatively charged residues at different *pH*s.

pH	Residue	Fractional charge (|e|)	Net protein charge (|e|)
4.8	Asp	-0.97	-0.25
	Glu	-0.80	
5.0	Asp	-0.97	-7.0
	Glu	-0.87	
5.2	Asp	-0.98	-12.0
	Glu	-0.91	
5.5	Asp	-1.0	-17.0
	Glu	-0.93	
6.0	Asp	-1.0	-22.0
	Glu	-0.98	
7.0	Asp	-1.0	-24.0
	Glu	-1.0	

In this model, a coarse–grained protein is composed of four types of CG beads (~ 2000 total beads per catalase enzyme). Two types of CG beads are used to represent the negatively charged residues (*Asp* and *Glu*). Since equal charges are assigned to positively charged residues (*Arg* and *Lys*), a single type of *CG* bead is used to represent them. The fourth type of bead represents the remaining types of amino acids. The electrostatic and the excluded volume interactions are included in the model. Since a larger population of hydrophobic residues are located within protein's core, we ignore non-electrostatic attraction in the model. The electrostatic interactions are computed using P^3M method[23] implemented in the *HOOMD*-blue package[24], which, does not account for charge regulation effects[25–27]. It could be an interesting future work to include these effects in addition to capturing the spatial distribution of protein charges and many body effects. And, we employ the *WCA* potential[28] to account for the excluded volume interaction between beads using eq.(1).

$$U_{WCA}(r) = \begin{cases} 4\varepsilon\left[\left(\frac{\sigma}{r}\right)^{12} - \left(\frac{\sigma}{r}\right)^{6}\right] + \varepsilon, & \text{if } r \le 2^{1/6}\sigma. \\ 0, & \text{otherwise.} \end{cases} \quad (1)$$

In equation (1), ε is the interaction strength, σ is a distance between two particles when the potential between them is 0 and r is the center to center distance between particles.

A schematic diagram of a protein adsorption study using a coarse grained *MD* approach is shown in fig.(1). We use a simulation box elongated along the y direction such that $L_x = L_z = L_y/3.0$. The box is centered at the origin. Then, we introduce a $2D$ charged surface, composed of alternately distributed cationic and neutral beads, at $y = -L_y/6.0$ plane in a simulation box. We apply periodic boundary conditions only in the x and z dimensions. For this purpose, we place a hard wall at $-L_y/2.0$ end of the box. This design sets up the distance between the charged surface and hard wall equal to $L_y/3$, which is equivalent to the $x-$ and $z-$ dimensions of the box. Then, proteins are randomly distributed in the region between the charged surface and hard wall. This setup

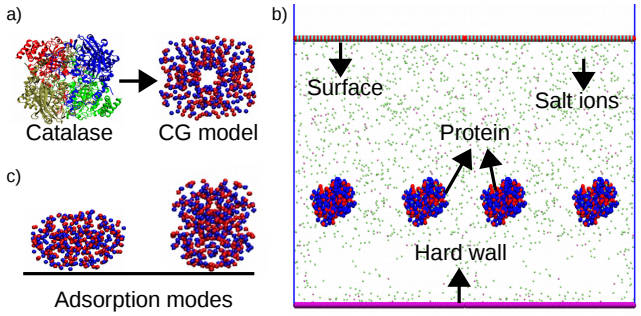

Fig. 1 Schematic of a protein adsorption study. a) Detail structure of a catalase enzyme (pdb: $1TGU$) and its coarse grained model. b) Simulation box containing a system of proteins, a charge embedded surface, a hard wall, and explicit salt ions. c) Two adsorption modes; one *via* the largest (termed here "flat on") and another *via* the smallest (termed "standing up") interface contact.

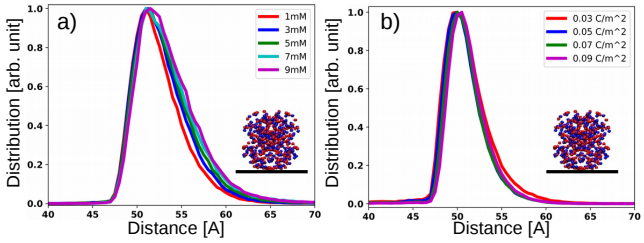

Fig. 2 Time–averaged distribution of the protein's centroid with respect to the distance: a) at various salt concentrations; b) at different surface charge densities. Distributions are normalized to 1. In both figures, the centroid is located ~ 52Å, which implies that the protein has adopted the "standing up" adsorption mode. The mode of protein adsorption is shown inside figures. The surface charge density in fig.(a) is $0.1C/m^2$. In fig.(b), salt concentration is $1mM$. Protein charge in both figures is $-12|e|$.

creates $\frac{2}{3}L_y$ empty space above the charged surface so that there will be a highly decayed electrostatic field of the charged surface on the wall. To achieve a neutral box, counterions are added in a protein free region in the box. A further addition of coion and counterion pairs in the box is required if a system has to satisfy the desired salt concentration. The box dimensions along x- and z- directions are 75 nm (L_x, L_z) each and y dimension is $3L_x$. The system size varies depending on parameters such as salt and protein concentrations, surface charge density, and protein charges. On average, simulation box consists of $200,000$ CG beads in our simulations. In our model, we ignore the conformational changes of proteins by treating them as rigid bodies; that is, we neglect changes in the folded conformation upon adsorption. After the simulation is set up, we first integrate a system of proteins and ions by utilizing the NVE integrator in $HOOMD$ to avoid possible overlaps between particles. Then, we use the Langevin dynamics integrator to move proteins, and ions within the box, obeying the potentials mentioned in the previous paragraph. We run simulations for 2×10^7 total time steps using 0.01 as a step size. In the real unit, the step size and total time steps correspond 5 fs and 100 ns, respectively. In this simulation time, we observe both the number of adsorbed proteins and total energy saturate.

3 Results and discussion

3.1 Preferential adsorption mode of the protein

We chose a low protein concentration to determine the adsorption preference of the protein. At lower concentrations, the preferential adsorption mode of the protein is independent of the protein–protein interaction. The probability distribution of the protein's centroid with respect to the distance from the charged surface is calculated to deploy as a parameter for analyzing the adsorption modes of proteins on the charged surface. In fig.(2), the time–averaged distributions of the protein's centroid with respect to the distance from the charged surface is shown for various salt concentrations, and surface charge densities. The peaks of each distribution, which represents the distance of the centroid from the charged surface, are located ~ 52Å away from the charged surface. Based on the dimensions of the catalase (100Å $\times$ 100Å $\times$ 75Å), this distance indicates that the protein is adsorbed onto the surface via its smallest (100×75) interface. Adsorption *via* the smallest interface (largest interface) is described as the "standing up" ("flat on") adsorption mode. Note that, in "standing up" mode, catalase covers ~ 1.33 times less surface area than in the "flat on" landing mode.

Although the Salt concentration was increased up to 10 mM, we did not find a complete adsorption mode transformation from the "standing up" to the "flat on" mode. The slight peak's width mismatch observed in the distribution is caused by a variation in the screening length at different salt concentrations. Similarly, the preferential adsorption mode is also found to be independent of the surface charge density. The peaks under each condition do however have broader widths suggesting that the adsorbed proteins are not immobilized on the surface. Next, we study the protein charge effects by keeping the surface charge density, and salt concentration constant at $0.1C/m^2$, and $1mM$, respectively. The time–averaged distribution of the catalase's centroid for different protein charges is shown in fig.(3a).

When the net protein charge is $-7|e|$, a peak with a broader width is observed at ~ 55Å from the charged surface. This distance indicates that the protein is adsorbed in the "standing up" mode. The overall net charge of the catalase protein is increased up to $-22|e|$, however we did not observe the "flat on" adsorption mode. With an increase in protein charges, the location of the peak shifts towards the charged surface. Instead of a complete adsorption mode transformation, we observe a tilting of the adsorbed protein making an angle up to ~ 50 degrees to the surface. Due to the tilting, there are mismatches between the positions of peaks at the different protein charges (fig.(3a)). The peaks are found to be separated by ~ 5A when the overall net protein charge is changed from -7 and $-22|e|$. Note that, this value would be ~ 12Å if proteins were adsorbed in the "standing up" mode at one charge and in the "flat on" mode at the another.

Our analysis suggests that the preferential adsorption mode of catalase ("standing up") is caused by a local interaction between the protein and the surface. To investigate this interaction, we plot the distribution of each charged residues as well as the overall net charge distribution with respect to the distance from the charged surface at various protein charges, which is shown in

fig.(3 b, c, and d). The overall net charge distribution (represented by the green color) is computed using the expression:

$$n(y) = \sum_r n_r(y) q_r. \quad (2)$$

Where $n_r(y)$ is the number of charged residues of the type r located at distance y from the surface, q_r is the partial charge of the residue, and the sum is performed over all charged residues. In the plot, there are a number of peaks and troughs in the distribution of overall net charges. Peaks in the distribution mean that the magnitude of the positive charges is larger than the magnitude of the negative charges, while troughs mean the opposite. Closer to the charged surface, there is a trough, which suggests that the protein in the "standing up" adsorption mode exhibits more negative residues to the positively charged surface. Thus, the "standing up" type of adsorption mode is favored by the local protein–surface electrostatic attraction.

Sub–plots (b, c, and d) in fig.3 also reveal that both the distributions of charged residues and the overall net charge distributions are slightly changed due to changes in the protein charges. The net charge distribution at $q = -7|e|$ is symmetric on either sides of the deepest trough. The deepest trough is essentially the location of the adsorbed protein's centroid. However, the distribution becomes more asymmetrical as the protein charge is increased. This is understood to be caused by the tilting of the adsorbed protein at the higher charges. The tilting of adsorbed proteins observed at the higher net protein charges increase the local attractive interaction between the "*Glu*" residues, and the surface and this, in turn, strengthens the adsorption. This also supports the observation of narrower peaks at the higher protein charges as shown in fig.(3a).

Both the Coulomb attraction between the surface and a protein, and the counterions release are contributing factors for the protein adsorption. We have analysed the role of counterions release/confinement on the protein adsorption. For this, the number of ions in the adsorbed proteins' monolayer (~ 105Å) as well as in the vicinity of the surface (~ 7Å) are compared before and after the protein adsorption. We find that the number of ions in the monolayer is reduced after the protein adsorption. This suggests that the release of counterions is one of the driving forces for protein adsorption. This is consistent with the counterions release attributed to the association of charged polymers to oppositely charged surfaces and/or oppositely charged colloids as well as the precipitation of proteins[29–31]. However, the population of negative ions in the region close to the charged surface (~ 7Å) increases after the protein adsorption. Negative ions in the layer, distributed over the charged surface, facilitates the proteins' adsorption. This is analogized to the confinement of counterions in cavities for neutralizing the aggregate of charged proteins[31,32]. The recruitment of more ions close to the surface is required if more proteins are adsorbed on the surface.

3.2 Protein assembly on the charged surface

Ordered assemblies of proteins have tremendous potential for bio–and nano– technological applications such as heterogeneous

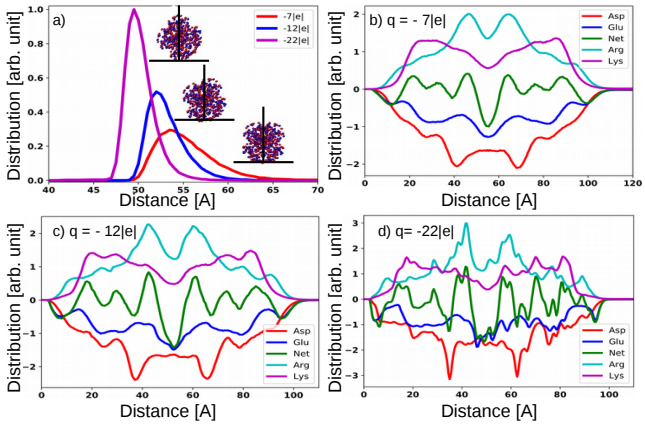

Fig. 3 Mode of protein adsorption and the resulting distributions of residues at various protein net charges. a) Location of the protein's centroid at various protein charges. The centroid of the protein having higher charges is closer to the surface due to a slight tilting of the adsorbed protein. The adsorption modes of protein at different protein charges is also shown in the figure. Distributions of individual residues and the overall net protein charges when $q = -7|e|$ (b), $q = -12|e|$ (c), and $q = -22|e|$ (d). In fig.(b), the net charge distribution (shown in green color) is identical on either sides of the deepest trough. However, the net charge distribution becomes more asymmetric as the charge is increased. This is due to the tilting of the adsorbed protein towards the surface. The surface charge density, and the salt concentration are kept constant at $0.1\ C/m^2$, and $1\ mM$, respectively.

catalysts, sensors, selective filters etc[15,33,34]. To control protein assembly on a surface, we fine–tune the concentration of protein in the solution. To characterize the structure of adsorbed proteins on a charged surface, we study the positional and angular correlations between the proteins. The positional correlation between adsorbed proteins is measured by calculating the probability distribution of the centroids of the adsorbed proteins. Similarly, the angular correlation parameter is determined locally by measuring the angle between adsorbed proteins located within a certain cutoff distance from a reference point. We treat the position of a protein as a reference point. As before, the probability distribution of the protein's centroid with respect to the distance from the charged surface is used as a parameter for analyzing the mode of protein adsorption on a surface.

3.2.1 Effects of protein concentration

Proteins adsorbed on the surface for different protein solution concentrations are shown in fig.(4). As expected, both low and high protein concentrations are unfavorable for yielding an ordered assembly on the surface. At low protein concentration (fig.4a), the quantity of the adsorbed proteins is low and proteins move in a non–correlated fashion on the surface. Note that, proteins adopt the "standing up" adsorption mode when the surface coverage is low. At higher concentrations, on the other hand, a larger population of the proteins accumulate closer to the surface (fig.4d), but the resultant structure is a disordered aggregate. In figure 4, an adjustment of protein adsorption mode can also be seen. Once the critical density of proteins on the surface is reached, the proteins change their adsorption from a solely "standing up" mode (observed at low concentration) to a combi-

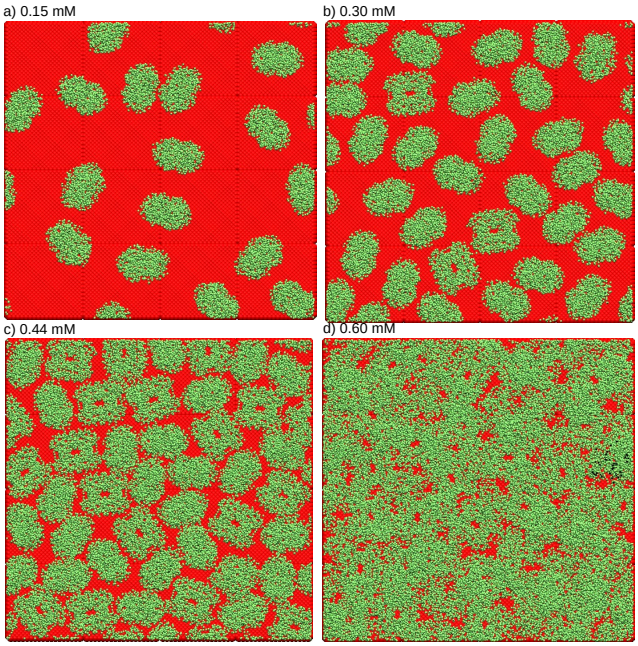

Fig. 4 Simulations snapshots showing protein adsorption conformations at 0.15 mM (a), 0.30 mM (b), 0.44 mM (c), and 0.60 mM (d) protein solution concentrations. Shown snapshots are in the xz plane. The salt concentration, protein charges, and surface charge density are kept constants at $1\ mM$, $-22|e|$, and $0.1C/m^2$, respectively.

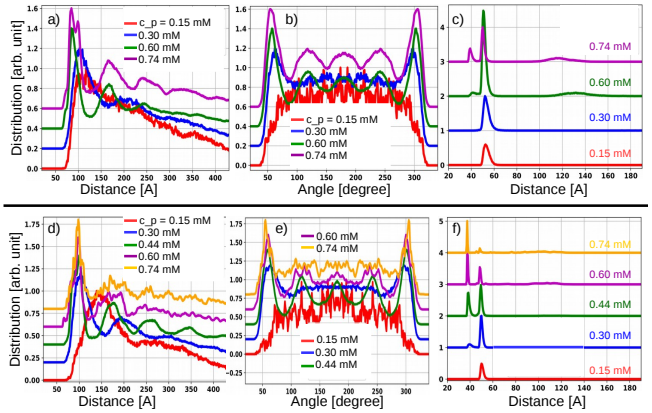

Fig. 5 Effect of protein concentration on the adsorption mode and the resulting protein assembly. Upper and lower panel figures correspond to $-12|e|$, and $-22|e|$ protein charges, respectively. a, d) Distributions of proteins' centroid–centroid distance at various protein solution concentrations. b, e) Angular distributions of proteins within a 120Å cut-off distance from a central protein. c, f) Concentration profiles of proteins' centroid with respect to the distance from a charged surface. For the comparison purpose, distributions corresponding to concentrations larger than $0.15mM$ are shifted vertically. Salt concentration and surface charge density are kept constants at $1\ mM$ and $0.1C/m^2$, respectively.

nation of "standing up" and "flat on" modes (fig.4b). In one experimental study, it was reported that these types of orientational changes were observed in the adsorption of lysozyme proteins on a silica surface[35]. The value of critical density depends on the charges of protein, salt concentration, and surface charge density.

In fig.(5), the effects of protein concentrations on the adsorption mode and $2D$ structure formed on the surface is analysed for protein charges $-12|e|$ (shown in upper panel) and $-22|e|$ (lower panel). The salt concentration, and surface charge density are kept constant at $1mM$, and $0.1C/m^2$ respectively and the protein concentration in the solution is varied from $0.15mM$ to $0.74mM$. Sub–plots (a and d) show the positional correlations between adsorbed proteins. Similarly, the angular correlation and adsorption modes are plotted in (b and e), and (c and f), respectively. Both the positional and the angular order parameters in fig.(5a, b, d, e) reveal that the structures are disordered for low and high concentrations of protein.

The order parameters at protein concentrations $0.60mM$, in the upper panel, and $0.44mM$, in the lower panel, indicate that the structures on the surface are comparatively correlated. The local angular order parameter shows that there are 5 distinct peaks separated by 60 degrees at these concentrations. This suggests that the protein is surrounded by six nearest neighbours, which is characteristic of a structure having hexagonal symmetry. Also, there are multiple peaks in the positional order parameter and their locations are comparable to the expected peak positions of a structure having hexagonal symmetry. Here, the peaks are not matched perfectly because, due to the charge heterogeneity and/or correlation effects, proteins do not strictly reside on fixed lattice sites. Instead they vibrate and change their alignment on the surface. The variation in the protein sites' separation is also caused by the adsorption of proteins in the different modes. The amount of fluctuation between inter–sites distance depends on the dimension of the protein molecule.

The probability distribution of the protein's centroid with respect to the distance from the charged surface is shown in fig.(5 c, and f). At low protein concentrations, the protein concentration profile has a single peak located at ~ 50Å, which means that the adsorbed proteins adopt the "standing up" adsorption mode. As the concentration of protein is increased further, another distinct peak around 38Å is observed. This peak is caused by the "flat on" adsorption mode. Proteins adsorb in a combination of the "standing up" and "flat on" type modes due to correlation effects. Based on the dimensions of the protein studied here, the separation between adsorbed proteins increases if they adsorb in the "flat on" mode. The population of the proteins adsorbed in the "flat on" mode rises when the proteins are highly charged and their concentration in the solution is large. In such conditions, proteins also form a second layer. Therefore, most proteins in the first layer chose the "flat on" adsorption mode for reducing their repulsion with other proteins in the first and second layers. The taller first peak at $0.6mM$ and $0.74mM$ protein concentrations in fig.(5 f) tells that a larger population of proteins in the first layer possess the "flat on" adsorption mode.

In fig.(6), proteins are adsorbed in a combination of "standing up" and "flat on" modes. We use this figure to demonstrate why "standing up" is preferred over the "flat on" type of adsorption mode in the case of the low surface coverage. The proteins adsorbed in the "flat on" mode are marked with green colored spheres. The positive and negative residues of proteins falling within 7Å of the charged surface are represented by small blue

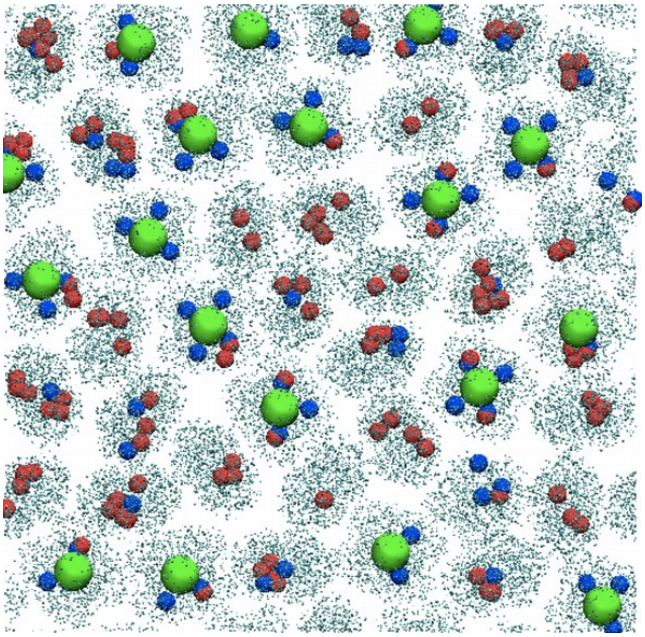

Fig. 6 Snapshot highlighting the charged residues of adsorbed proteins, which are within 7Å from the charged surface. Shown snapshot is in the xz plane. Negative and positive residues are represented by red and blue spheres respectively. For the comparison purpose, the centroid of molecules adsorbed in the "flat on" mode are marked by green spheres. In the "flat on" adsorption mode, molecules exhibit more positive residues (blue beads) close to the positively charged surface. Whereas, in the "standing up" mode, molecules display more red colored beads (negative residues) close to the surface.

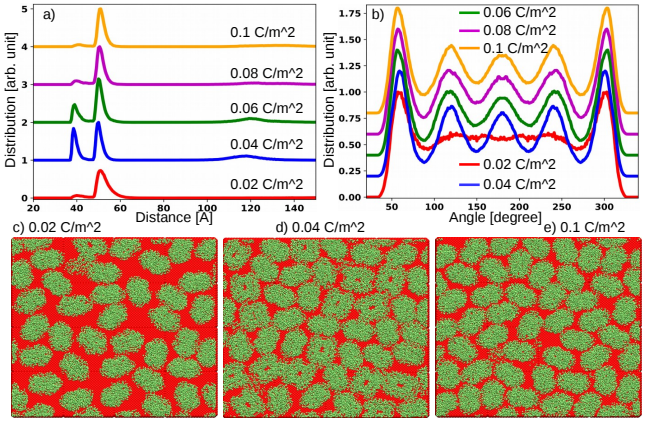

Fig. 7 Effect of surface charge density on mode of adsorption and protein assembly. a) Time–averaged distribution of proteins' centroid with respect to the distance. Both at low and high surface charge densities, distributions have a single peak. Whereas, at the intermediate values, there are two peaks. b) Angular distributions of proteins within a 120Å cutoff distance from a central protein at various surface charge densities. For the comparison purpose, distributions corresponding to surface charge densities larger than $0.02C/m^2$ are shifted vertically. c, d, e) Snapshots of protein assembly at $0.02C/m^2$, $0.04C/m^2$, and $0.1C/m^2$ surface charge densities. Shown snapshots are in the xz plane. Salt concentration, protein concentration, and protein net charge are $1\ mM$, $0.6mM$, and $-12|e|$, respectively.

and red spheres, respectively. In the "flat on" type of protein adsorption, there are more positive residues than negative residues closer to the surface. On the other hand, the "standing up" mode displays more negative residues to the surface. Since the "flat on" mode exhibits more positive residues close to the positively charged surface, this mode is electrostatically unfavorable.

As the adsorption of proteins increases, the proteins get laterally correlated by changing from "standing up" to a mixed "flat on" and "standing up" conformation. In such mixed state they develop some local order reminiscent of a crystal in $2D$ (we note that $2D$ crystals do not have long range order but only local order)[36,37]. The laterally correlated structure results when the protein adsorption nearly cancels the charge of the surface and is correlated because of the repulsion between the proteins. If one protein is removed, a hole in the surface is cancelled by the neighboring proteins. This is similar to the correlated two–dimensional structure that results when multi–valent ions adsorb to strongly charged surfaces to cancel the surface charge in salt-free conditions[38]. As mentioned earlier, adsorbed proteins are not immobilized on surfaces, they change alignments to find the lowest free energy conformation, which is achieved by structures that have larger correlations (more lateral order) since correlations always decrease the free energy of the system[39].

3.2.2 Effects of surface charge density

In fig.(7a), the time–averaged protein concentration profiles with respect to the distance for different charge densities are shown. The protein charges, salt, and protein solution concentrations are kept constant at $-12|e|$, $1mM$, and $0.6mM$, respectively. The surface charge density is varied between $0.02C/m^2$ and $0.1C/m^2$. We observe that the adsorption mode is a complicated function of the surface charge density. When the surface charge density is $0.02C/m^2$, two peaks separated by ~ 12Å appear in the protein concentration profile. These peaks are the outcome of the proteins' adsorption in a combination of the "standing up" and "flat on" modes. However, the majority of the adsorbed proteins are "standing up" since the second peak is taller than the first peak. Due to a weak attractive interaction between surface and protein, the resulting protein structure is poorly correlated, which can be seen in fig.(7b, c).

When the surface charge density is in a range of $0.03 - -0.05C/m^2$, the first and the second peaks in fig (7a) are almost identical suggesting that half of the adsorbed proteins are in the "flat on" mode and the rest are in the "standing up" type of adsorption mode. This adsorption mode adjustment gives rise to an ordered structure having hexagonal symmetry (fig 7d). Above $0.05C/m^2$, the first peak diminishes and the second peak becomes taller again. In the $0.05C/m^2 - 0.1C/m^2$ surface charge density range, a larger quantity of proteins are adsorbed on the surface because of the stronger attractive force. To accommodate more proteins on the surface, they adsorb *via* their smallest interface. In this range of charge density, proteins on the surface are also assembled into a hexagonal structure, however, the inter–protein distance is smaller compared to the previous case. When the protein charge is increased to $q \sim -20|e|$, we obtain the ordered structures only at the low surface charge density regime ($0.04C/m^2$). At higher charge densities, we find the disordered aggregates.

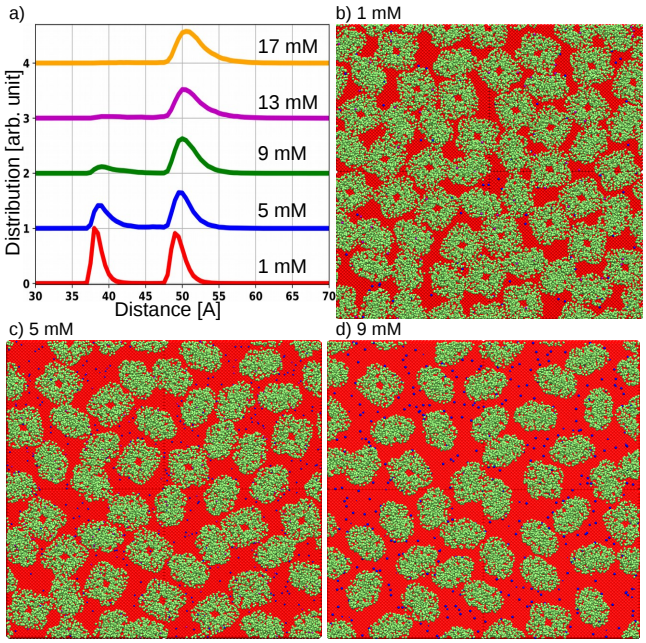

Fig. 8 Effects of salt concentration on adsorption mode and protein assembly. a) Time–averaged distribution of proteins' centroid for different salt concentrations. Snapshots of protein assembly at 1 mM (b), 5 mM (c), and 9 mM (d), respectively. Shown structures are in the xz plane. The surface charge density, protein concentration, and protein charges are $0.04\ C/m^2$, 0.4 mM, and $-22|e|$, respectively.

3.3 Effects of salt concentration

The concentration profile of proteins with respect to the perpendicular distance from the charged surface is shown in fig.(8a). We vary the salt concentration from $1mM$ to $20mM$ in the interval of $4mM$ by keeping the protein charges, protein concentration, and the surface charge density constants at $-22|e|$, $0.44mM$, and $0.04C/m^2$, respectively. With an increase in salt concentration, we notice two major changes in the concentration profile. First, the peak located closer to the surface slowly disappears, which means that the "flat on" mode of adsorption is unfavorable at high salt concentrations. Secondly, the magnitude of the adsorbed proteins diminishes. This suggest that correlations dominate at low salt in a mixed "standing up" and "flat on" conformations.

For small salt concentrations, the electrostatic interactions are weakly screened. Therefore, proteins are adsorbed onto the surface with mixed adsorption modes (8b, c) to reduce repulsion and build correlations. At high salt concentrations, the electrostatics is weakened. Also, the entropy gain due to counterions release is small. Thus, the number of adsorbed proteins declines with an increase in salt concentration. As a result of a weak lateral repulsion between proteins on the surface, proteins are favorable to retain their preferred adsorption mode ("standing up") at higher salt concentrations (8d).

As we see in fig.(8b), which corresponds to $1mM$ salt concentration, proteins are densely populated on the surface and most proteins are surrounded by six nearest neighbours in the structure. When the salt concentration is increased to 5 mM, the $2D$ structure is transferred into a less dense structure (fig.8c). Above 10 mM salt concentrations, the correlation between adsorbed proteins becomes very weak because of a decline in the protein density on the surface. When the salt concentration is increased from 1 mM to 10 mM, the screening length ($\lambda = \frac{3.05[\text{Å}]}{\sqrt{c_0[M]}}$) is decreased from ~ 100Å to ~ 30Å, approximately by a factor of 3. Even though the electrostatic interactions are strong at 10 mM, the quantity of adsorbed proteins decreases due to the adsorption of more counterions on the charged surface. In our study, we observe a thin layer of negative ions (counterions of the surface) on the charged surface in addition to the adsorbed proteins. This observation is supported by a recent experimental study by Miller et al.[40]. While they have reported a well–ordered distribution of counterions on the charged surface, we have only characterized the protein assembly on the charged surface. Accumulation of counterions near the charged surface decreases the effective surface charge density, which, in return, decreases the protein adsorption. Note that the counterions release is entropically unfavorable at higher salt concentrations.

We observe disordered structures when the surface charge density is high ($> 0.1C/m^2$) and/or protein is strongly charged (attraction is too strong). Furthermore, non–correlated structures (fluid like) are observed when the surface charge density is below $0.02C/m^2$ (too weak attraction). We find ordered assembly in a wide range of surface charge density ($0.025C/m^2 - 0.1C/m^2$) when proteins are weakly charged. When proteins are strongly charged ($\sim -20|e|$), we observe ordered assembly only at smaller surface charge density values $\sim 0.04C/m^2$. Ordered $2D$ assemblies, in our study, are formed when interactions are both not too weak and/or strong. These observations are consistent with previous studies, which report the requirements of a right solution condition and/or interactions range for protein crystallization and ordered assemblies[41–44]. People have classified protein–protein attraction into specific and non–specific and drawn phase diagram with respect to the strength of these interactions[44]. We have protein–surface and protein–protein electrostatic and excluded volume interactions in our study (non–specific type of interactions). Please note that we have explicit salt ions in the model too. However, hydrogen bonding, disulfide bonding (specific interactions) as well as water are not captured in our CG model. A competition between protein–protein and protein–surface interaction mediated by ions determines an adsorption mode and protein assembly on surfaces. Protein-surface attraction is responsible for driving proteins to the surface. Then, non-specific interactions play crucial roles in adjusting contacts, alignments and orientations of proteins to give rise to $2D$ structures.

Standing up and flat on configurations can generally be expected in proteins having distinct dimensions at least in two directions. Adsorption interface of proteins depends on number of parameters including a protein specific parameter, residues distribution. Choosing catalase as a model protein, we identify its adsorption interface. Then, study how various parameters affect the modes of adsorption and resulting assemblies. One of the nice feature of this model is that it captures a spatial distribution of protein residues. Therefore, this model can be applied (and extended) for other proteins such as Albumins, Globulins, Fibrinogens (blood proteins), to name a few, to study adsorption

modes and assemblies. The generalities of the results are various: at low salt concentrations, as the degree of adsorption increases (by changing the overall protein concentration), a correlated $2D$ structure will form to decrease the free energy (please recall that the free energy can be expressed as an ideal part plus correlations and therefore correlations always decrease the free energy). The only condition is that the proteins have charged residues randomly distributed on the surface as oppose to large domains of positive and negative groups (indeed, the analysis of various protein surfaces show rather small charged domains, randomly distributed on their surface[45]. Also, it is general that as the salt concentration increases, the proteins will de-adsorb because the correlations get screened by the salt and now the surface charge is also suppressed by the salt ions.

4 Conclusions

Here, we study protein adsorption and structure formation on surfaces at various parameter settings such as surface charge density, salt concentration, protein concentration, and protein charge and distribution. By accounting for the heterogeneous charge distribution in the model, we find that the preferential adsorption mode of the catalase protein is *via* its smallest interface ("standing up" orientation) at low protein adsorption. The preferential adsorption mode of the protein is governed by the local electrostatic interactions between the surface and heterogeneously distributed protein residues. The Coulomb attraction between the surface and protein and the counterions release are two contributing factors for protein adsorption. The electrostatic attraction between the protein and surface drives the protein to the surface. Once the protein reaches the charged surface, local electrostatic interactions between the surface, and the residues of the protein come into play. The interaction between the positively charged surface, and the negatively charged residues of proteins supports the adsorption, while the local repulsion between the surface, and the positively charged residues are favorable for breaking proteins apart from the surface. The spatial distribution of charged residues on the protein surface and many body interactions, which are often ignored in theoretical/simulation studies, play a major role in determining the modes of protein adsorption and the types of protein assembly on the charged surface.

By increasing the protein solution concentration, we find the critical protein density on the surface for modifying the modes of protein adsorption. The critical density relies on parameters such as surface charge density, salt concentration, and protein charges. As the density of adsorbed protein is increased on the surface, a correlation between adsorbates starts to build. As a result of which, some adsorbed proteins adjust their adsorption mode from "standing up" to "flat on". Moreover, even when adopting the same adsorption mode, proteins change their alignment to build correlations. The modification of adsorption modes and alignments is attributed to the inter–protein repulsion. The changes in the binding modes and orientations induce changes in the $2D$ protein structure on the surface.

When the surface charge density is increased, the adsorption mode of proteins is found to change from the "standing up" to a "mixed" (a combination of "standing up" and "flat on") and back to "standing up" mode. These changes induce the structural transformation of the $2D$ protein assembly from a poorly correlated sparse $2D$ structure to a densely packed ordered structure having hexagonal symmetry. At low surface charge, the attractive force for the adsorption is weak. As a result, the quantity of the protein is small and all proteins are adsorbed in the "standing up" mode, their electrostatically preferred adsorption mode. The surface charge density increment attracts additional proteins to the surface and proteins adjust their modes of adsorption to configure a densely packed $2D$ structure with hexagonal symmetry. With the further increase in the surface charge density ($\sim 0.1C/m^2$), proteins are found to prefer the "standing up" mode again, yielding the hexagonal symmetry having relatively the smaller lattice constant than at the smaller surface charge densities. For a weakly charged protein ($\sim -10|e|$), we observe ordered protein assemblies in a wide range of surface charge density values ($0.04C/m^2 - 0.1C/m^2$). However, when the proteins are strongly charged ($\sim -20|e|$), we observe ordered structures only at low surface charge densities ($\sim 0.04C/m^2$). In the case of salt concentration, the correlated surface structure melts as the salt concentration increases because the charged surface is cancelled by the salt ions and the proteins de–adsorb. This study provides guidelines for controlling the modes of protein adsorption and protein assembly on surfaces.

Conflicts of interest

“There are no conflicts to declare”.

Acknowledgements

This work was supported by the Department of Energy, Basic Energy Science grant number DE-FG02-08ER46539, and by the Sherman Fairchild Foundation.

References

1 R. Chelmowski, A. Prekelt, C. Grunwald and C. WÃűll, *The Journal of Physical Chemistry A*, 2007, **111**, 12295–12303.
2 A. W. Sonesson, T. H. Callisen, H. Brismar and U. M. Elofsson, *Colloids and Surfaces B: Biointerfaces*, 2008, **61**, 208–215.
3 K. C. Dee, D. A. Puleo and R. Bizios, *An Introduction to Tissue-Biomaterial Interactions*, 2002, p. 248.
4 L.-C. Xu, J. W. Bauer and C. A. Siedlecki, *Colloids and Surfaces B: Biointerfaces*, 2014, **124**, 49–68.
5 I. H. Jaffer, J. C. Fredenburgh, J. Hirsh and J. I. Weitz, *Journal of Thrombosis and Haemostasis*, 2015, **13**, S72–S81.
6 J. West and J. Moon, *Current Topics in Medicinal Chemistry*, 2008, **8**, 300–310.
7 K. Wang, C. Zhou, Y. Hong and X. Zhang, *Interface Focus*, 2012, **2**, 259–277.
8 F. Hofmeister, *Archiv für experimentelle Pathologie und Pharmakologie*, 1888, **24**, 247–260.
9 A. A. Green, *Journal of Biological Chemistry*, 1931, **93**, 517–542.
10 C. Tanford, *Physical Chemistry of Micromolecules*, John Wiley & Sons, Hoboken, NJ, 1961.

11 F. Fang and I. Szleifer, *Biophysical Journal*, 2001, **80**, 2568–2589.

12 J. Zhou, J. Zheng and S. Jiang, *The Journal of Physical Chemistry B*, 2004, **108**, 17418–17424.

13 F. Carlsson, E. Hyltner, T. Arnebrant, M. Malmsten and P. Linse, *The Journal of Physical Chemistry B*, 2004, **108**, 9871–9881.

14 F. Fang, J. Satulovsky and I. Szleifer, *Biophysical Journal*, 2005, **89**, 1516–1533.

15 M. Rabe, D. Verdes and S. Seeger, *Advances in Colloid and Interface Science*, 2011, **162**, 87–106.

16 R. Sugadev, D. Balasundaresan, M. Ponnuswamy, D. Kumaran, S. Swaminathan and K. Sekar, *RCBS Protein Data Bank*, 2005.

17 P. Chelikani, I. Fita and P. C. Loewen, *Cellular and Molecular Life Sciences (CMLS)*, 2004, **61**, 192–208.

18 J. Kaushal, S. Mehandia, G. Singh, A. Raina and S. K. Arya, *Biocatalysis and Agricultural Biotechnology*, 2018, **16**, 192–199.

19 J. D. Brodin, E. Auyeung and C. A. Mirkin, *Proceedings of the National Academy of Sciences*, 2015, **112**, 4564–4569.

20 M. X. Wang, J. D. Brodin, J. A. Millan, S. E. Seo, M. Girard, M. Olvera de la Cruz, B. Lee and C. A. Mirkin, *Nano Letters*, 2017, **17**, 5126–5132.

21 K. Krishnamoorthy, K. Hoffmann, S. Kewalramani, J. D. Brodin, L. M. Moreau, C. A. Mirkin, M. Olvera de la Cruz and M. J. Bedzyk, *ACS Central Science*, 2018, **4**, 378–386.

22 G. R. Grimsley, J. M. Scholtz and C. N. Pace, *Protein Science*, 2009, **18**, 247–251.

23 D. N. LeBard, B. G. Levine, P. Mertmann, S. A. Barr, A. Jusufi, S. Sanders, M. L. Klein and A. Z. Panagiotopoulos, *Soft Matter*, 2012, **8**, 2385–2397.

24 J. A. Anderson, C. D. Lorenz and A. Travesset, *Journal of Computational Physics*, 2008, **227**, 5342–5359.

25 W. M. de Vos, F. A. M. Leermakers, A. de Keizer, M. A. Cohen Stuart and J. M. Kleijn, *Langmuir*, 2010, **26**, 249–259.

26 G. S. Longo and I. Szleifer, *Journal of Physics D: Applied Physics*, 2016, **49**, 323001.

27 F. M. Boubeta, G. J. A. A. Soler-Illia and M. Tagliazucchi, *Langmuir*, 2018, **34**, 15727–15738.

28 J. D. Weeks, D. Chandler and H. C. Andersen, *The Journal of Chemical Physics*, 1971, **54**, 5237–5247.

29 Bruinsma, R., *Eur. Phys. J. B*, 1998, **4**, 75–88.

30 H. Schiessel, R. F. Bruinsma and W. M. Gelbart, *The Journal of Chemical Physics*, 2001, **115**, 7245–7252.

31 Y. R. Dahal and J. D. Schmit, *Biophysical Journal*, 2018, **114**, 76–87.

32 J. D. Schmit, S. Whitelam and K. Dill, *The Journal of Chemical Physics*, 2011, **135**, 085103.

33 A. L. Margolin and M. A. Navia, *Angewandte Chemie International Edition*, 2001, **40**, 2204–2222.

34 T. Ueno, *Chemistry - A European Journal*, 2013, **19**, 9096–9102.

35 S. M. Daly, T. M. Przybycien and R. D. Tilton, *Langmuir*, 2003, **19**, 3848–3857.

36 J. M. Kosterlitz and D. J. Thouless, *Journal of Physics C Solid State Physics*, 1972, **5**, L124–L126.

37 B. I. Halperin and D. R. Nelson, *Phys. Rev. Lett.*, 1978, **41**, 121–124.

38 I. Rouzina and V. A. Bloomfield, *The Journal of Physical Chemistry*, 1996, **100**, 9977–9989.

39 J. Hansen, I. R. Mcdonald and D. Henderson, *Physics Today*, 1988, **41**, 89–90.

40 M. Miller, M. Chu, B. Lin, M. Meron and P. Dutta, *Langmuir*, 2015, **32**, 73–77.

41 A. George and W. W. Wilson, *Acta Crystallographica Section D Biological Crystallography*, 1994, **50**, 361–365.

42 S. Whitelam, Y. R. Dahal and J. D. Schmit, *The Journal of Chemical Physics*, 2016, **144**, 064903.

43 M. F. Hagan and D. Chandler, *Biophysical Journal*, 2006, **91**, 42–54.

44 S. Whitelam, *Phys. Rev. Lett.*, 2010, **105**, 088102.

45 T. D. Nguyen, B. Qiao and M. O. D. L. Cruz, *Proceedings of the National Academy of Sciences*, 2018, **115**, 6578–6583.